Science of Sintering, **50** (2018) 467-476

doi: https://doi.org/10.2298/SOS1804467M

UDK 546.62; 621.78.063

Alumina Particles Doped With Ferric as Efficient Adsorbent for Removal of Reactive Orange 16 from Aqueous Solutions

Predrag Milanović[1], Marija M. Vuksanović[2*)], Miodrag Mitrić[3], Aleksandar Kojović[1], Dušan Mijin[1], Radmila Jančić-Hainemann[1]

[1]University of Belgrade, Faculty of Technology and Metallurgy, Karnegijeva 4, 11000 Belgrade, Serbia

[2]University of Belgrade, Innovation Center of Faculty of Technology and Metallurgy, Karnegijeva 4, 11000 Belgrade, Serbia

[3]University of Belgrade, Institute of Nuclear Sciences "Vinča", P.O. Box 522, 11001 Belgrade

Abstract:

Ferric oxide doped alumina particles were prepared via the sol-gel method and their performance as Reactive Orange 16 adsorbent was evaluated. The concentrations of the Reactive Orange 16 were monitored using a UV–Vis spectrophotometer. The effect of Reactive Orange 16 concentration, adsorbent quantity and pH on the solution decolorization efficiency was analyzed. The efficiency of the Reactive Orange 16 removal using ferric oxide alumina doped exceeded 98 % in 20 min at pH=3. The experimental data were fitted to the Langmuir equation better than to the Freundlich one. The pseudo-first-order model fits well with the experimental data for adsorption kinetics.

Keywords*: Ceramic fibers; Adsorption; Reactive Orange 16.*

1. Introduction

Water pollution is one of the most studied problems in the present time. Textiles industries are using large amount of dies and a part of that quantity is find in the waste waters. Azo dyes are among the pollutants that have high impact in the environment and it is important to remove them from the waste water. Reactive Orange 16 (C.I. 17757) is anionic monoazo reactive dye ($C_{20}H_{17}N_3Na_2O_{11}S_3$, MW=617.54 g/mol) which is used in textile industry for dying cotton or viscose fibers. It is highly soluble in water (120 g/L at 20 ^oC) and due to that can be present in textile effluents. Image 1 shows the structural formula of this die [1]. There have been significant works in finding the best way for removing heavy metals from water, by using alumina as adsorbent [2], as well as for azo dyes [3]. It is shown that the rate of the sorption process on alumina is different for metal ions and dyes [4].

One of the main goals nowadays is the synthesis of inorganic metal oxides with large surface areas, which could be used as adsorbents or catalysts [5]. The forms of the adsorbent varies from ordered structures, ceramic fibers or powders [6]. The form that has the best mechanical properties is corrundum, but is rather poor as the adsorbent and is mostly used as the reinforcement in composite materials [7, 8].

In the present study, alumina particles doped with ferric oxide were prepared by sol-gel technique and their adsorption characteristic for the removal of the Reactive Orange 16

*) **Corresponding author:** mdimitrijevic@tmf.bg.ac.rs

(RO16) dye from aqueous solution was studied. The adsorption experiments were carried out so as to measure the effect of contact time, pH, adsorbent dose and initial concentration variations were explored in batch experiments, as well as form of adsorbent. The adsorption isotherm and kinetic studies were also carried out to estimate the adsorption mechanism [9].

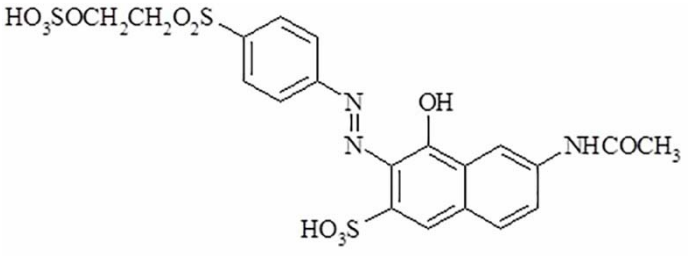

Fig. 1. Structure of reactive orange 16 one of the azo dies used in textile industries.

2. Experimental Procedures

2.1. Materials

Aluminium hydroxide chloride (Locron L; $Al_2(OH)_5Cl{\cdot}2{,}5\ H_2O$) was purchased in the crystallized state from the Clariant company. Reactive Orange 16, textile dye, was obtained from Sigma Aldrich (dye content 50 %) and used without purification. Deionised water was obtained from a Milipore Waters Milli-Q purification unit. Iron chloride ($FeCl_3{\cdot}6H_2O$), used as a source of iron ions, was obtained from Sigma-Aldrich.

2.1. Preparation of alumina particles

The sol-gel procedure was used for the preparation of alumina based ceramic particles. Two series of particles were prepared. Water solution of aluminium chloride hydroxide with addition of $FeCl_3$ as the ferrous oxide precursor was prepared as the water solution [10]. Then the obtained solution was poured into a petri dish and left to form a gel. The gels were grinded and the particles were heat treated at 700 ºC and 900 ºC during 2 h in air.

2.2. Characterization of particles

The X-ray powder diffraction was performed using a Bruker D8 Advance diffractometer in Bragg-Brentano transmission mode θ/θ with the primary germanium (Ge (111)) monochromator of Johannson type ($CuK\alpha_1$ radiation). Anodic voltage and anodic current were 40 kV and 30 mA, respectively. The diffraction data were collected by using scintillation counter of NaI (TI) type and the scan-step method in the range of 2θ diffraction angle from 10-90º, with step size of 0.05º and counting time of 6 s per step.

2.3. Decolorization procedure of reactive orange 16 dye

The concentrations of the RO16 were determined using UV-Vis Shimadzu 1700 spectrophotometer, at 493 nm. The dye removal from aqueous solutions was investigated in a series of experiments. Standard solution of the RO16 dye was prepared by dissolving 30 mg of the RO16 dye in 0.5 L of deionized water. The pH of the solution was adjusted by the addition of dilute solution of HCl or NaOH. For a typical experiment, 50 mL of prepared solution was taken and the volume of the mixture was adjusted to 100 mL with deionized

water and steered at 500 rpm. After pH adjustment the alumna ferous oxide doped particles were added. The sampling was done at the interval of 5 min, centrifuged for 1 min at 6000 rpm using SpectrafugeMini centrifuge and analyzed by UV-Vis spectrophotometer.
The decolorization efficiency (DE%) was calculated with the following equation:

$$DE(\%) = \frac{A_i A_t}{A_i} \cdot 100 \quad (1)$$

where A_i, is the initial absorbance of the dye solution and A_t is the absorbance at time t [11].
The adsorption capacity at equilibrium, q_e (mg/g), was calculated using the following equation:

$$q_e = \frac{(C_o - C_e)V}{m} \quad (2)$$

where C_0 is the initial dye concentration (mg/L), C_e is the dye concentration at equilibrium (mg/L), V is the volume of dye solution used (L), and m is the mass of the adsorbent used (mg) [12].

2.4. Adsorption kinetic models

In order to understand the adsorption process of RO16, two kinetic models including pseudo-first-order and pseudo-second order models were selected to fit the kinetic data [11].
Pseudo first order and pseudo second order rate equations [10] were used to analyze the kinetic data. The linear form of the pseudo-first-order models is given by:

$$q_t = q_t\left(1 - e^{-k_1 t}\right) \quad (3)$$

where q_t and q_e are the amounts of the dye adsorbed at time, t, and at equilibrium, respectively, and k_1 is the pseudo first order rate coefficient.
The pseudo second order model can be declared as [13]:

$$q_t = \frac{k_2 q_e^2 t}{1 + k_2 q_e t} \quad (4)$$

where k_2 is the pseudo second order rate coefficient.

2.5. Equilibrium studies

Kinetic experiments were performed at concentrations of 15, 30, 45 and 60 mg/L of the RO16. At each concentration a 100 mg of particles were placed in dye solution and at the proper time intervals the absorbance was determined. The amount of the adsorbed RO16 was calculated as mentioned [14].

The adsorption isotherm was determined at equilibrium with a fixed pH. Experiments were conducted with different concentration of the RO16 and fixed metal oxide loading (100 mg particles).

The adsorption capacity of particles is simulated by Langmuir isotherms [15]:

$$q_e = \frac{Q_{\max} b C_e}{1 + b C_e} \quad (5)$$

and Freundlich isotherms [15]:

$$q_e = K C_e^n \quad (6)$$

Here, C_e is the equilibrium concentration of the solute in the bulk solution mg/L, q_e is the amount of solute adsorbed per unit mass of adsorbent at equilibrium mg/g, Q_{max} is the maximum monolayer adsorption capacity in mg/g, b is the Langmuir constant in L/mol, and K and n are the Freundlich isotherm constants [16].

Langmuir model could be presented in linearized form:

$$\frac{C_e}{q_e} = \frac{\frac{C_e}{q_{\max+i}}}{bq_{\max}} \tag{7}$$

and Freundlich model in linearized form:

$$\log q_e = \log K_F + \frac{1}{n}\log C_e \tag{8}$$

3. Results and Discussion

The decolorization rate of the dye solutions with ferric oxide doped alumina particles was investigated. The effect of the initial pH, adsorbent loading and the initial dye concentrations on adsorption was studied.

3.1. Characterization of particles

The XRD patterns of particles obtained from the precursor with the addition of $FeCl_3$ are shown in Fig. 2:

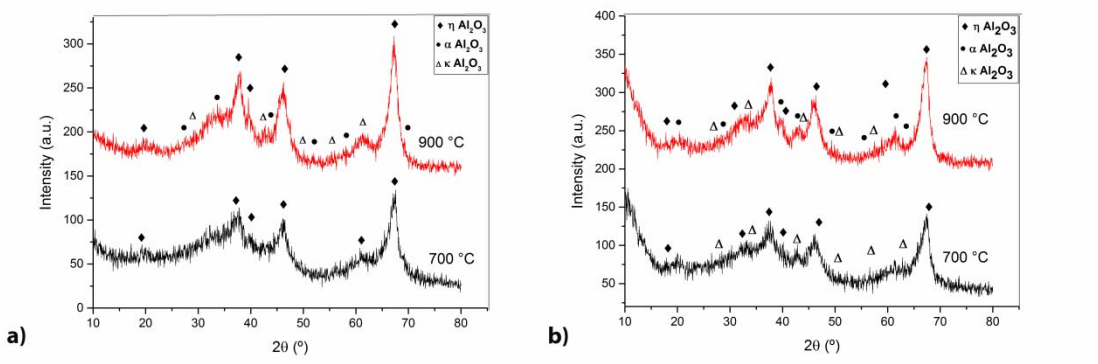

Fig. 2. XRD of the particles after heat treatment at 700 °C and 900 °C a) particles without the addition of $FeCl_3$ b) particles with the addition of $FeCl_3$

According to Fig. 2a in the alumina based particles treated at 700 °C there was eta – Al_2O_3 (PDF-2 77-0396) detected. With temperature increase to 900 °C the dominant phases are η – Al_2O_3 (PDF-2 77-0396), κ – Al_2O_3 (PDF-2 73-1199) and α - Al_2O_3 (PDF-2 74-1081), about 18 %. The XRD patterns of the synthesized ferric oxide doped alumina particles after heat treatment at 700 °C and 900 °C are shown in Fig. 2b. At 700 °C the dominant phases are η – Al_2O_3 (PDF-2 77-0396) and κ – Al_2O_3 (PDF-2 73-1199). In alumina particles doped with iron heated at 900 °C the dominant phases are η – Al_2O_3 (PDF-2 77-0396), κ – Al_2O_3 (PDF-2 73-1199) and corundum (PDF-2 74-1081), about 25 %. This indicates that the addition of ferrous oxide eases the formation of corundum.

3.2. Adsorption

The set of experiments were performed at different pH (3, 4, 5 and 9) and without additional pH adjustments (pH 6.5) in order to determine the adsorption properties of samples for dye removal at present system (100 mL of solution, 30 mg/L dye concentration, 25 °C, 150 mg of sample).

3.3. Effect of adsorbent

The adsorbent dosage is considered as one of the most effective parameters in the adsorption process. Fig. 3 shows that higher decolorization efficiency is obtained at samples that are prepared at lower calcination temperature. The addition of ferrous oxide didn't prove to be an efficient way of increasing the adsorption capacity of the material. The addition of ferrous oxide facilitates the formation of corund structure that is less effective as the adsorbent compared to eta and kappa phases. The structure of corundum phase is less open than the structure of other phases [17]. On the other hand the particles having corundum in their structure are the easiest to manipulate and have good properties in manipulation and enable the preparation of the material that is easy to handle. Therefore, the adsorbent with the added Fe treated on 900 °C was selected for further experiments. It was interesting to find the conditions for the possible use of this adsorbent as it is a possible good material to obtain a sintered structure of the adsorbent that will enable the scale up of the process.

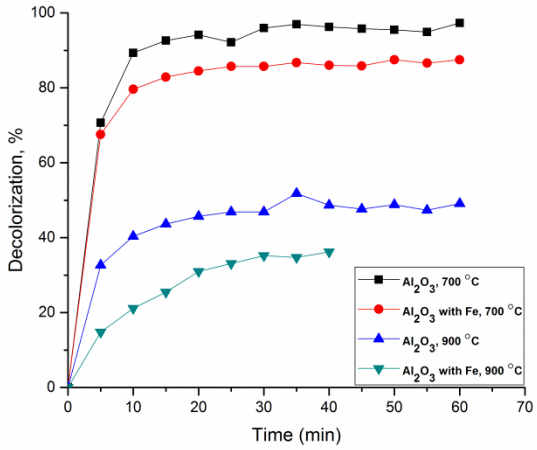

Fig. 3. Decolorization efficiency at (150 mg particles, pH 6.5 volume 100 ml and concentration 30 mg/L RO16).

3.4. The pH influence on the RO16 dye adsorption

The influence of different pH values on the RO16 dye removal is shown in Fig. 4. Obtained results show that the dye molecules removal depends on pH values, and the RO16 dye removal efficiency is increased when the pH value of the solution decreases.

The maximum removal of RO16 dye adsorption, even nearly 99 %, was achieved when pH values are in the range from pH 3 to pH 4. The similar trend of pH effect was reported for the adsorption of anionic dyes [18,19]. The influence of pH on the RO16 removal efficiency presumably is due to its influence on the surface properties of the adsorbent and ionization/dissociation of the adsorbate molecule. For pH value less than 5, protonation of functional groups is occurred, and the electrostatic interaction between the positively charged adsorbent surface and the negatively charged dye molecules increases [20].

At higher values, between pH 5 to pH 9, the excess OH^- ions and deprotonation of functional groups cause reduced interactions between the adsorbent and adsorbate, and adsorption is limited. Due to the electrostatic repulsion, a negatively charged surface site on the adsorbent doesn't favor the adsorption of the anionic RO16 dye molecules [20, 21].

A similar observation has been reported for the adsorption of the anionic dye, Methyl Orange on alumina particles which is strongly governed by the aqueous pH. Additionally, it was estimated that the pH of 2.5 is the optimum pH for which the adsorbent efficiency for the removal of dye is maximum [22].

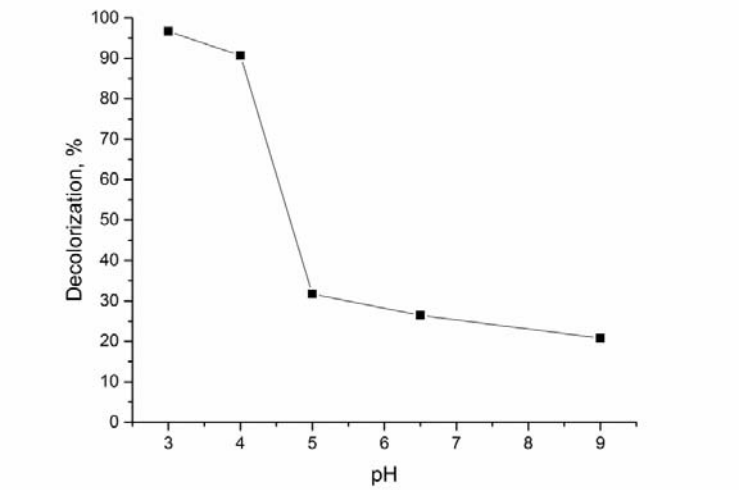

Fig. 4. The influence of pH on the RO16 dye removal efficiency (100 mg particles, volume 100 mL and concentration 30 mg/L RO16).

3.5. Effect of adsorbent mass on the RO16 dye adsorption

To investigate the effect of adsorbent dosage at pH 3, the amount of adsorbent was varied in the range of 50–1000 mg/L (Fig. 5). The maximum decolorization efficiency of the RO16 at pH 3 was recorded after 20 min and it was > 98 % at the dosage of 200 mg which was the fastest process to attain equilibrium. The same efficiency was obtained in the final result using only 100 mg of the adsorbent but the time required for adsorption was slightly longer. The point of further optimization will be to choose between two demands: to achieve the high adsorption level in a short time or achieve the same elimination of the die using less adsorbent and more time. The proposed material could be studied in those two hypotheses.
The time required to reach equilibrium is relatively short compared to the literature data (and shorter than 1h) and it is highly dependent on the mass of the added adsorbent. According to the literature review, for the dyes whose particles are much more expanded (bigger) than the metal ones, the process is slower and the time required to reach equilibrium is much longer. For C.I. Acid Orange 7 it is equal to 360 min, for C.I. Reactive Black 5 and C.I. Direct Blue 71 the equilibrium time is 240 min. [6].

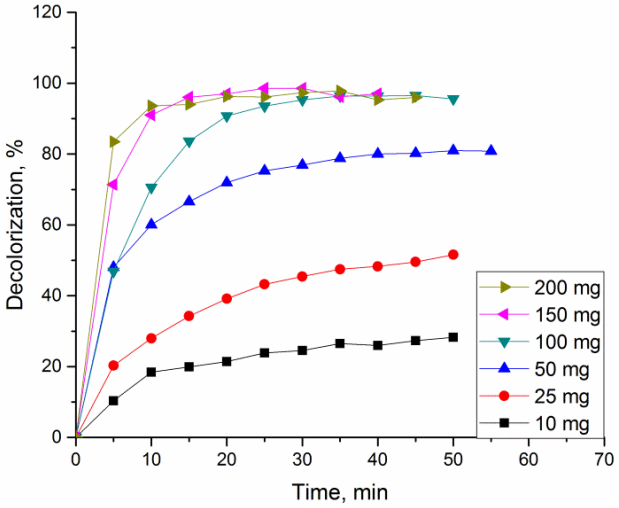

Fig. 5. Effect of adsorbent mass on the RO16 dye adsorption (pH 3, volume 200 ml and concentration 30 mg/L of RO16).

3.6. Analysis of the sorption mechanism

The results of fitting with adsorption isotherm models are listed in Table I. The fitting was done by usage of linearized form of Langmuir and Freundlich isotherms, as it was done by other authors [16]. According to the obtained correlation coefficients the experimental equilibrium data were fitted to the Langmuir isotherm (R^2=0.996). Fitting the processes by the Freundlich model results in a middle level of confidence (R^2 = 0.935).

Tab. I Obtained isotherms constants for adsorption of RO16.

Isotherm	Qmax, mg/g	b, L/mol	K_f, L/mg	n	R^2
Langmuir	10.4	1.47	-	-	0.996
Freundlich	-	-	4.52	3.91	0.935

The Langmuir isotherm assumes monolayer adsorption onto the homogenous surface containing a finite number of adsorption sites with no transmigration of the adsorbate in the plane surface. Once a site is occupied, no further adsorption can take place at that site. This indicates that the surface reaches a saturation point where the maximum adsorption of the surface is achieved [7, 23].
The same type of saturated adsorption was reported for the adsorption of RO16 on porous chitosan–polyaniline/ZnO hybrid composite [20], and Methyl Orange on mesoporous alumina nanofibers prepared by electrospinning from aqueous solutions [16] as well for other azo dyes [19, 21]. Some studies indicate that the adsorption of the RO16 dye was due to the chemical interactions [20].

3.7. Adsorption kinetic modelling

Kinetic data were fitted to the pseudo first-order and pseudo second-order kinetic models(Fig. 6). Adsorption rate constants and their correlation coefficients were calculated by non-linear fitting experimental data and they are summarized in Table II. The fitting was done in batch mode using mathematical tools to minimize normalized sum of the squares of the errors in original equations (Equation 3 and Equation 4) by finding optimal parameters values (k_1, k_2). The validity of the models was checked by the correlation coefficient (R^2), and the calculated equilibrium adsorption capacities appeared that the pseudo first-order model was fit well with the experimental data.

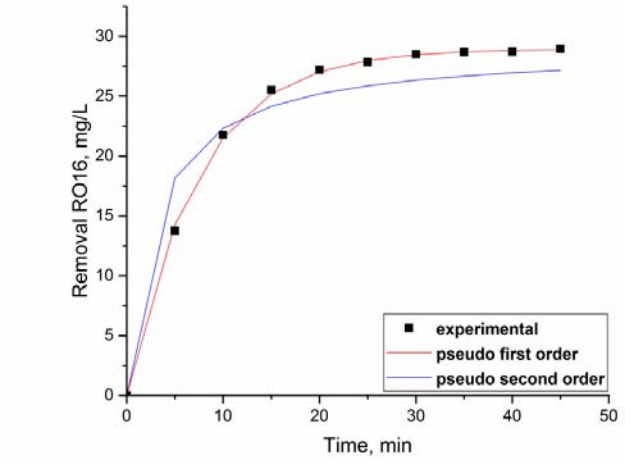

Fig. 6. Fitting for RO16 adsorption kinetic modeling based on pseudo first-order and pseudo second-order kinetic models equations (pH 3, 100 mg particles, volume 100 ml and concentration 30 mg/L RO16).

The adsorption correlation coefficient R^2 was approximately close to one, which fits the experimental data to pseudo first-order better than the pseudo second-order for the adsorption process. Therefore, it can be concluded that pseudo first-order equation is better in describing the adsorption kinetics of RO16 on alumina particles. Several earlier workers have shown that pseudo-second-order model fits well in describing the adsorption process. The pseudo-second order model suggests that the adsorption depends on the adsorbate as well as the adsorbent and involves chemisorptions process in addition to physisorption [20]. It has to be highlighted that, according to the literature, it could be expected that the kinetics of removal of dye with alumina are described with pseudo second-order equation is better in describing the adsorption kinetics [4, 16, 22, 24] and that calculated correlation coefficient R^2 for those adsorptions for pseudo second-order was 0.97-0.99. Due to high number of experimental data that should be processed, mathematical tool [25-27] for batch calculation of coefficients by optimizing parameters was used, while most of other researchers fitted linearized form of equations for kinetic modes. The cross-check was done by fitting linearized forms of equations and the similar values for coefficients were obtained, but the values for correlation coefficient were significantly different.

Tab. II Fitting parameters for RO16 adsorption kinetic modeling based on pseudo first-order and pseudo second-order kinetic model equations.

Sample	k_1	R^2	k_2	R^2
150mg Al_2O_3 with Fe treated at 700 °C (pH 6,5, 30mg/L RO16)	6.826	0.9742	0.042	0.9964
150mg Al_2O_3 treated at 700 °C (pH 6,5, 30mg/L RO16)	6.837	0.9651	0.026	0.9954
150mg Al_2O_3 treated at 900 °C (pH 6,5, 30mg/L RO16)	0.222	0.9922	0.056	0.9841
150mg Al_2O_3 with Fe treated at 900 °C (pH 3, 30mg/L RO16)	10.100	0.9354	0.037	0.9972
100mg Al_2O_3 with Fe treated at 700 °C (pH 6,5, 30mg/L RO16)	0.100	0.9979	0.020	0.9855
100mg Al_2O_3 with Fe treated at 700 °C (pH 6,5, 30mg/L RO16)	0.156	0.9993	0.022	0.9797
200mg Al_2O_3 with Fe treated at 700 °C (pH 6,5, 30mg/L RO16)	7.394	0.9794	0.060	0.9934
150mg Al_2O_3 with Fe treated at 700 °C (pH 3, 30mg/L RO16)	0.158	0.9996	0.014	0.9825
150mg Al_2O_3 with Fe treated at 900 °C (pH 3, 30mg/L RO16,500 ml H_2O_2)	7.435	0.9642	0.033	0.9909
100mg Al_2O_3 with Fe treated at 900 °C (pH 3, 30mg/L RO16,500 ml H_2O_2)	0.138	0.9997	0.009	0.9890
200mg Al_2O_3 with Fe treated at 900 °C (pH 3, 30mg/L RO16,500 ml H_2O_2)	8.782	0.9883	0.061	0.9961
50mg Al_2O_3 with Fe treated at 900 °C (pH 3, 30mg/L RO16,500 ml H_2O_2)	0.143	0.9931	0.015	0.9933
25mg Al_2O_3 with Fe treated at 900 °C (pH 3, 30mg/L RO16,500 ml H_2O_2)	0.076	0.9965	0.011	0.9843
100mg Al_2O_3 with Fe treated at 900 °C (pH 3, 30mg/L RO16,1000 ml H_2O_2)	0.136	0.9997	0.012	0.9806
100mg Al_2O_3 with Fe treated at 900 °C (pH 3, 30mg/L RO16,300 ml H_2O_2)	0.082	0.9916	0.005	0.9729
100mg Al_2O_3 with Fe treated at 900 °C (pH 3, 30mg/L RO16,200 ml H_2O_2)	0.164	0.9992	0.015	0.9827
100mg Al_2O_3 with Fe treated at 900 °C (pH 3, 30mg/L RO16,100 ml H_2O_2)	0.156	0.9999	0.013	0.9836
100mg Al_2O_3 with Fe treated at 900 °C (pH 3, 30mg/L RO16)	6.106	0.9357	0.022	0.9836
100mg Al_2O_3 with Fe treated at 900 °C (pH 4, 30mg/L RO16)	0.191	0.9991	0.019	0.9816
100mg Al_2O_3 with Fe treated at 900 °C (pH 5, 30mg/L RO16)	0.071	0.9838	0.015	0.9793
100mg Al_2O_3 with Fe treated at 900 °C (pH 6,5, 30mg/L RO16)	0.108	0.9801	0.031	0.9868

100mg Al_2O_3 with Fe treated at 900 °C (pH 9, 30mg/L RO16)	0.073	0.9834	0.026	0.9705
10mg Al_2O_3 with Fe treated at 900 °C (pH 6,5, 30mg/L RO16)	0.033	0.9815	0.037	0.9455
10mg Al_2O_3 with Fe treated at 900 °C (pH 3, 30mg/L RO16)	0.087	0.9927	0.020	0.9887
10mg Al_2O_3 with Fe treated at 900 °C (pH 3, 30mg/L RO16)	0.094	0.9979	0.025	0.9841
100mg Al_2O_3 with Fe treated at 900 °C (pH 9, 30mg/L RO16)	0.073	0.9834	0.026	0.9705
10mg Al_2O_3 with Fe treated at 900 °C (pH 6,5, 30mg/L RO16)	0.033	0.9815	0.037	0.9455
100mg Al_2O_3 with Fe treated at 900 °C (pH 6,5, 30mg/L RO16)	0.070	0.9904	0.021	0.9812
100mg Al_2O_3 with Fe treated at 900 °C (pH 6,5, 30mg/L RO16)	0.034	0.9930	0.015	0.9701
100mg Al_2O_3 with Fe treated at 900 °C (pH 6,5, 30mg/L RO16)	0.103	0.9959	0.021	0.9737

4. Conclusion

Alumina particles and alumina with ferrous oxide content were prepared by the sol–gel methods using aluminium chloride hydroxide as a precursor and $FeCl_3$ as the precursor for ferrous oxide. Two different sintering temperatures were used, 700 °C and 900 °C. The thus-produced alumina particles were characterized by XRD. Based on the results of the XRD, the alumina particles with doped Fe calcined at 900 °C were identified with content of α-alumina phase as 25 wt.%. In addition, a series of phase transitions such as eta →kappa→α-alumina were observed on 700 °C and 900 °C.

Adsorption kinetic data were analyzed by the first- and second-order kinetic equations. The adsorption property of RO16 of the α- and γ-alumina particles was better described on the basis of the pseudo first-order rate mechanism. The fitting was done using mathematical tools for optimization on original form of equations. According to literature review, it could be expected that experimental results better fit to second-order mechanism of adsorption.

Acknowledgments

This research has been financed by the Ministry of Education, Science and Technological Development of the Republic of Serbia as a part of the projects TR34011.

5. References

1. Zaharia Carmen and Suteu Daniela, Textile Organic Dyes, Dr. Tomasz Puzyn (Ed.), (2012) 56.
2. A. Rahmani, H. Z. Mousavi and M. Fazli, Desalination., 253 (2010) 94.
3. E. Khosla, S. Kaur and P. N. Dave, J. Eng., 2013 (2013) 1.
4. M. Wawrzkiewicz, M. Winiewska, A. Woowicz, V. M. Gunko and V. I. Zarko, Micropor. Mesopor. Mat., 250 (2017) 128.
5. A. Golubović, B. Simović, S. Gašić, D. Mijin, A. Matković, B. Babić, M. Šćepanović, Sci. Sinter. 49 (2017) 319.
6. A. Drah, N. Z. Tomić, Z. Veličić, A. D. Marinković, Ž. Radovanović, Z. Veličković and R. Jančić-Heinemann, Ceram. Int., 43 (2017)13817.
7. F. A. Alzarrug, M. M. Dimitrijević, R. M. J. Heinemann, V. Radojević, D. B. Stojanović, P. S. Uskoković and R. Aleksić, Mater. Design, 86 (2015) 575.

8. Adela Egelja, Jelena Majstorović, Nikola Vuković, Miroslav Stanković, Dušan Bučevac, Sci. Sinter. 48 (2016) 303.
9. M. Cocić, M. Logar, B. Matović, S. Dević, T. Volkov – Husović, S. Cocić, V. Tasić, Sci. Sinter. 48 (2016) 197.
10. P. Milanović, M. Vuksanović, M. Mitrić, D. Stojanović, A. Kojović, J. Rogan and R. Jančić Heinemann, Sci. Sinter., 50 (2018) 77.
11. E. Ghasemi, H. Ziyadi, A. M. Afshar and M. Sillanpää, Chem. Eng. J., 264 (2015) 146.
12. B. Yahyaei and S. Azizian, Chem. Eng. J., 209 (2012) 589.
13. S. Azizian, J. Colloid Inter. Sci., 276 (2004) 47.
14. K. S. Bharathi, S. T. Ramesh, Appl. Water Sci., 3 (2013) 773.
15. J. Shen, Z. Li, Y.-n. Wu, B. Zhang and F. Li, Chem. Eng. J., 264 (2015) 48.
16. R. Istratie, M. Stoia, C. Pcurariu and C. Locovei, Arab. J. Chem. (2016) 1.
17. S. Agarwal, I. Tyagi, V. K. Gupta, M. H. Dehghani, J. Jaafari, D. Balarak and M. Asif, J. Mol. Liq., 224 (2016) 618.
18. V. Janaki, B.-T. Oh, K. Shanthi, K.-J. Lee, A. K. Ramasamy and S. Kamala-Kannan, Synthetic Met., 162 (2012) 974.
19. P. Kannusamy and T. Sivalingam, Colloid Surface B., 108 (2013) 229.
20. Y. Iida, T. Kozuka, T. Tuziuti and K. Yasui, Ultrasonics., 42 (2004) 635.
21. S. Banerjee, S. Dubey, R. K. Gautam, M. C. Chattopadhyaya and Y. C. Sharma, Arab. J. Chem. (2017) (In Press) https://doi.org/10.1016/j.arabjc.2016.12.016.I.
22. Langmuir, J. Am. Chem. Soc., 40 (1998) 1361.
23. S. Lan, N. Guo, L. Liu, X. Wu, L. Li and S. Gan, Appl. Surf. Sci., 283 (2013) 1032.
24. http://commons.apache.org/proper/commons-math/.
25. J. Feng, X. Hu, P. L. Yue, H. Y. Zhu and G. Q. Lu, Ind. Eng. Chem. Res., 42 (2003) 2058.
26. E. Neyens and J. Baeyens, J. Hazard. Mater., 98 (2003) 33.
27. V. S. Munagapati, V. Yarramuthi and D.-S. Kim, J. Mol. Liq., 240 (2017) 329

Садржај: *Честице на бази алуминијум оксида допиране гвожђе оксидом припремљене су сол-гел методом и процењена су њихова својства као адсорбента реактивне боје (Reactive Orange 16). Концентрације реактивне боје (Reactive Orange 16) праћене су коришћењем UV – видљивог спектрофотометра. Анализиран је утицај концентрације реактивне боје (Reactive Orange 16), количине адсорбента, pH, време деколоризације и ефикасност деколоризације раствора. Ефиксаност деколорицазије реактивне боје (Reactive Orange 16) коришћењем честица на бази алуминијум оксида допираних гвожђем оксидом прелази 98% у временском периоду од 20 минута. Експериментални подаци су боље постављени у Лангмуирову једначину него у Френдлихову. Модел псеудо – првог реда добро одговара експерименталним подацима за кинетику адсорпције.*
Кључне речи*: Керамичке честице, Адсорпција, Реактивна боја (Reactive Orange 16).*